OBIC Technique Applied to Wide Bandgap Semiconductors from 100 K up to 450 K

Hassan Hamad, Dominique Planson, Christophe Raynaud, Pascal Bevilacqua

OBIC Technique Applied to Wide Bandgap Semiconductors from 100 K up to 450 K

H Hamad, D Planson*, C Raynaud, P Bevilacqua
Univ Lyon, INSA, CNRS AMPERE, F-69100, VILLEURBANNE, France.
E-mail: dominique.planson@insa-lyon.fr

Abstract. Wide bandgap semiconductors have recently become more used in the power electronics domain. They are predicted to replace the traditional silicon especially for high voltage and/or high frequency devices. Device design has shown a big progress in the last two decades. Substrates up to six inches of diameter are now commercialized with very low defect densities. Such a development is due to many studies that never stop. Among these studies, the ones that allow an excess of charge carriers in the space charge region (like OBIC-Optical Beam Induced Current- and EBIC-Electron Beam Induced Current-) are efficient to analyze the variation of electric field as function of the voltage and the beam position. This paper shows OBIC technique applied to wide bandgap semiconductors based devices. OBIC cartography gives an image of the electric field in the device, and the analysis of OBIC signal help determining some characteristics of the semiconductors like minority carrier lifetime and ionization rates. These are key parameters to predict device switching behavior and breakdown voltage.

1. Keywords
OBIC technique, photon generation, wide bandgap semiconductors, electric field, minority carrier lifetime, ionization coefficients, temperature dependence of ionization rates.

2. Introduction

Power electronic devices based on wide bandgap (WBG) semiconductors (like silicon carbide SiC, gallium nitride GaN, diamond C ...) offer better performances when compared to those based on the silicon Si. Higher critical electric field, lower intrinsic charge carrier density, and higher saturation velocity are critical characteristics that make from devices based on WBG semiconductors a good choice to replace the silicon that has reached its technical limits. Therefore, WBG devices show higher breakdown voltage, they can operate under higher temperatures (up to 600 °C), and they present lower switching losses when integrated in power modules [1-2]. Nowadays, 4H-SiC and GaN devices (MOSFET and Schottky diodes) showing breakdown voltage up to 1200V, are commercialized [3-4]. Bipolar diodes and JFET with a breakdown voltage higher than 20 kV have been also realized [5]. However, there is a big gap between the theoretical performances and experimental ones for the WBG based power electronic devices. So, more studies are needed to improve some parameters as breakdown voltage and charge carrier lifetime. Electro-optical characterization of devices helps determining the spatial distribution of electric field as a function of the reverse voltage and the device doping profile. This paper shows the OBIC (optical beam induced current) technique applied to WBG semiconductor devices. Firstly, a theoretical approach is given to present the method. Experimental benches with two different wavelengths are described, and then, the different measurements and results are shown. The main aim of OBIC measurements is to determine ionization rates of free carriers in the semiconductor; a key parameter that help predicting breakdown voltage. Spatial distribution of the electric field gives a feedback about the performance of the junction termination protection. The determination of the minority carrier lifetime using OBIC is important to predict device dynamic behavior.

3. Theoretical Approach

When a semiconductor is illuminated perpendicularly with an optical beam, photons can interact with semiconductor electrons. Depending on the semiconductor bandgap (E_G) and the incident wavelength (λ), there are many results that can be reached.

In case of short wavelengths, photon energy ($E_\varphi = hC/\lambda$) will be much higher than E_G ($E_\varphi >> E_G$). Photon-electron interaction allows electron to gain energy and to pass to the conduction band. That leads to generate an electron-hole pair (EHP). Photon absorption follows in this case empiric Beer-Lambert law given in Eq. 1.

$$\frac{d\varphi}{dz} = -\alpha\varphi \qquad \text{Eq. 1}$$

where φ is the optical flux at a depth z in the semiconductor, and α is the single-photon absorption coefficient in the semiconductor.

For longer λ, E_φ will be much lower than E_G ($E_\varphi << E_G$), single-photon absorption is neglected, and then mutli-photon absorption takes place. M. Goeppert Mayer was the first one to predict two-photon absorption process in 1931 for $E_\varphi < E_G < 2*E_\varphi$ [6]. Optical flux and two-photon absorption coefficient β are related together as shown in Eq. 2.

$$\frac{d\varphi}{dz} = -\beta\varphi^2 \qquad \text{Eq. 2}$$

For $E_\varphi \lesssim E_G$, both processes can happen at the same time, Eq. 3 rules the absorption process in this case.

$$\frac{d\varphi}{dz} = -\beta\varphi^2 - \alpha\varphi \qquad \text{Eq. 3}$$

Table 1 shows generation type as a function of incident wavelength λ and the semiconductor.

Table 1. Photon absorption process for different wavelengths and materials.

Wavelength	**UV**				**Visible**		
λ [nm]	**100**	**200**	**300**	**400**	**500**	**600**	**700**
Si	Single-photon generation						
GaN	Single-photon generation			365	Two-photon generation		
4H-SiC	Single-photon generation			376	Two-photon generation		
6H-SiC	Single-photon generation			414	Two-photon generation		
Diamond	Single-photon	228	Two-photon generation		455	Three-photon generation	

If there is no electric field, generated EHPs will diffuse and any effect will not be observed. In order to highlight photon absorption, material should be submitted to an electric field. Figure 1 shows then a reverse biased PN junction. Once it is illuminated with a laser beam, electron-hole pairs (EHP) are generated. EHPs generated inside the space charge region (SCR) are submitted to an electric field. They are separated, and they reach the anode (holes) and the cathode (electrons). An optical beam induced current OBIC is then measured. For high reverse voltage, the SCR is submitted to higher electric field, generated EHPs acquire kinetic energy and they lead to generate new EHPs by collisions. Avalanche is reached when the number of generated EHPs becomes higher than the recombination rate. EHPs generated far outside the SCR will diffuse and recombine without any effect. EHPs generated outside the SCR may join it if the distance separating them is lower than the charge carrier diffusion length.

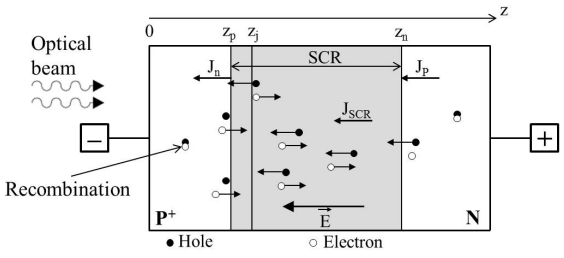

Figure 1. Generation of EHPs in a reverse biased PN junction illuminated with an optical beam.

In case of single-photon absorption process ($E_\varphi > E_G$), OBIC is a linear function of the optical flux. In this case two-photon absorption process ($E_\varphi < E_G < 2*E_\varphi$), OBIC is a quadratic function of the optical flux. This behavior was shown on 4H-SiC using a green laser source in 2014 (figure 2) [7].

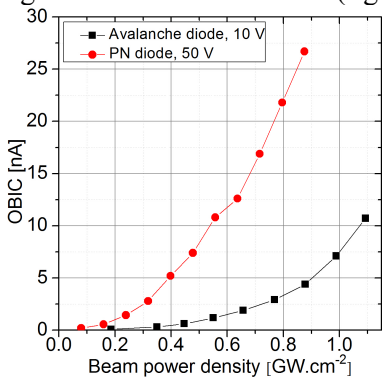

Figure 2. OBIC vs. beam power density on 4H-SiC bipolar diodes using a green laser beam.

4. Experimental setup

Two different laser sources are used in order to realize one- and two-photon OBIC measurements. First one is a UV laser (349 nm), and the second one is a green laser (532 nm). UV laser source is a pulsed source with a variable repetition frequency (up to 5 kHz) and pulse duration of about 4 ns. Pulse energy is controlled up to 120 µJ (30 kW of instantaneous power). Green laser is a pulsed laser with a repetition frequency of 20 kHz and pulse duration of about 1 ns. Pulse energy is controlled up to 5 µJ (5 kW of instantaneous power). Optical beam is guided through two semi-reflecting mirrors and a focusing lens of 100 mm focal distance. Mirrors and lens have rectilinear motions due to translation motors. Latters are controlled via LABVIEW interface to insure the position of the laser spot on the device under test (DUT). DUT is put in vacuum chamber allowing high voltage biasing insured using a Keithley 237 Source Measurement Unit (SMU). Figure 3 shows a general view of OBIC bench.

DUT is reverse biased during OBIC measurements, so measured current is the summation of OBIC and the leakage current I_l. OBIC signal is then deduced as the difference between total current and I_l. I_l must be low to not mask OBIC since it is a parasite signal.

With such parameters for the laser beam, when interrupting the optical beam, the generated current in the structure decreases immediately to its dark value. So, the local heating effect can be neglected, since thermal effects should lead to a slower decrease.

DUT structures are shown in figure 4. Structure (a) is a MESA protected 4H-SiC avalanche diode with optical window obtained using SIMS technique [8] (figure 4a). The optical window is a square of 100*100 mm^2. These diodes have high doping levels, and then SCR is submitted to high electric field (up to 5 MV/cm). Their breakdown voltage is about 59 V. Structure (b) is a JTE protected square PN diode with a breakdown voltage of 800 V (figure 4b). Low doping N layer is a 7 µm thick epitaxial layer. JTE layer is obtained by ion implantation and it is about 200 µm length. Figure 4c shows N-Schottky GaN pseudo-vertical structure. GaN layer is deposited on silicon substrate (structure c). These diodes have a breakdown voltage of 600 V but the leakage current of these diode is relatively high, so OBIC measurements are realized at low reverse voltage. P-Schottky diamond pseudo-vertical diodes (structure d) are also studied using OBIC technique. These diodes are MESA protected and they offer a breakdown voltage of 1 kV (figure 4d). Measurements on diamond diodes are realized using UV laser, so two-photon OBIC is measured in this case. OBIC measurements realized on 4H-SiC (and GaN) using green laser are based on two-photon absorption process. Ones realized using UV laser are based on single-photon absorption process.

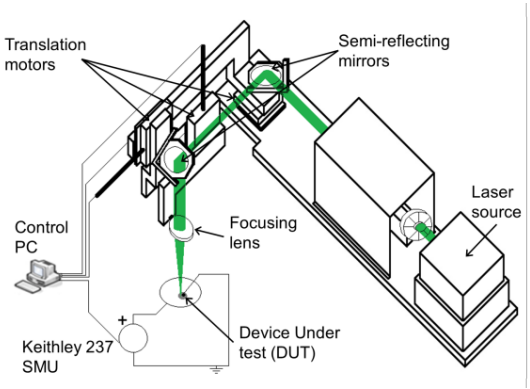

Figure 3. General view of OBIC bench.

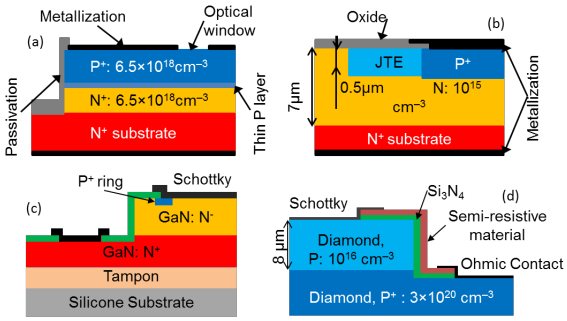

Figure 4. Partial cross section view of test devices. (a) Avalanche 4H-SiC diode, (b) JTE protected 4H-SiC bipolar diode, (c) N-Schottky pseudo-vertical GaN diode, (d) P-Schottky pseudo-vertical diamond diode.

5. Electric field imagery

OBIC measurements are realized by scanning the diode with the laser beam. Figure 5 shows OBIC signal (using UV laser source) measured on a diode (structure b) for a fixed reverse voltage of 100 V. An OBIC signal exists only when the optical beam illuminates the JTE of the diode. When the optical beam illuminates the metallization (reflecting surface) or outside the JTE, no current is measured. This result is in good agreement with the theory since the SCR (where a high electric field exists) is under the JTE.

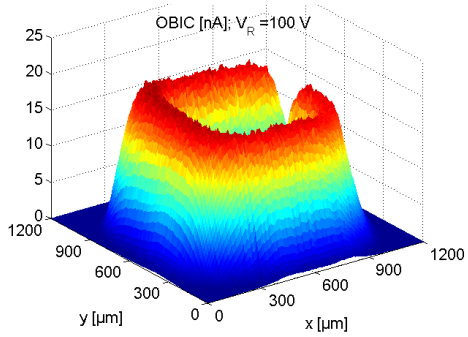

Figure 5. OBIC signal as a function of beam position for V_R = 100V obtained on structure b (4H-SiC) with the UV laser

These OBIC measurements help determining the efficiency of junction lateral protection. A constant OBIC signal at the edge of SCR means that electric field has the same profile in all the SCR which is well realized and it is adapted to applied reverse voltage. However, if the JTE is not well doped, OBIC peaks are measured at the edge of the JTE. Figure 6 shows an OBIC simulation, using 2D- simulation by finite elements on a JTE protected diode. The JTE is voluntary low doped in order to make a non-uniform electric field in the SCR. A peak of electric field at the recovery P^+/P region is manifested as a peak of OBIC current in the simulation [9].

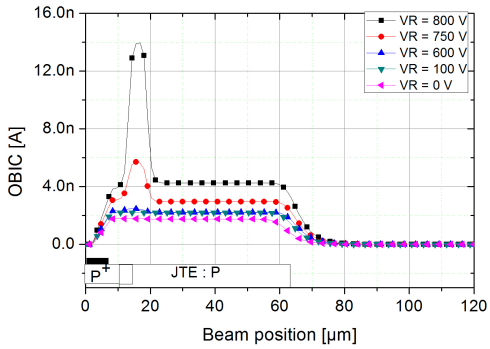

Figure 6. OBIC simulation on a low doped JTE protected diode, using the UV laser.

Spatial distribution of electric field is studied using OBIC technique in the diodes of structure b. Figure 7 shows OBIC versus beam position for several reverse voltages. For $V_R \leq 700$ V, OBIC is almost constant along the JTE, for higher voltage biasing, an OBIC peak appears at the edge of the P^+ region. Results mean that carrier multiplication is triggered at the edge of P^+ region and that this voltage is near V_{BR}.

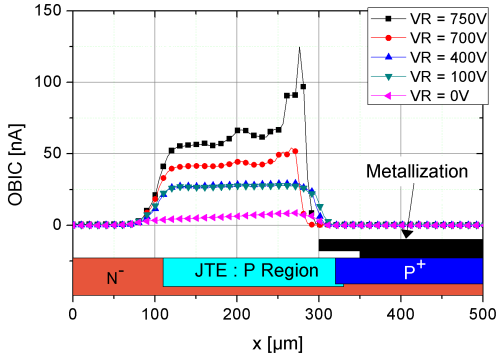

Figure 7. OBIC vs. beam position for several voltage reverse voltages (structure b) using the green laser.

OBIC measurements allow also detecting material defects. A defect is shown as a local variation of electric field. Figure 8 shows 2D-OBIC measurements on a diode with a defect. This diode has a breakdown voltage of 300 V. A local OBIC peak appears at the defect position, so OBIC technique is a non-destructive method to determine defects.

Other electric field studies are realized on GaN Schottky diodes (structure c). These are test measurements and they are realized under low reverse voltage biasing. The biggest problem when studying GaN diodes is the current collapse delay after an optical beam illuminates the material; in fact, an OBIC signal is observed, but it takes few seconds (up to 2 minutes depending of the diode) to reach the dark current. Figure 9 shows 2D-OBIC cartography for low reverse voltage (V_R = 10 V). Measurements are realized with a delay of 10 s. Results show an OBIC signal appearing only between the two metallization [10].

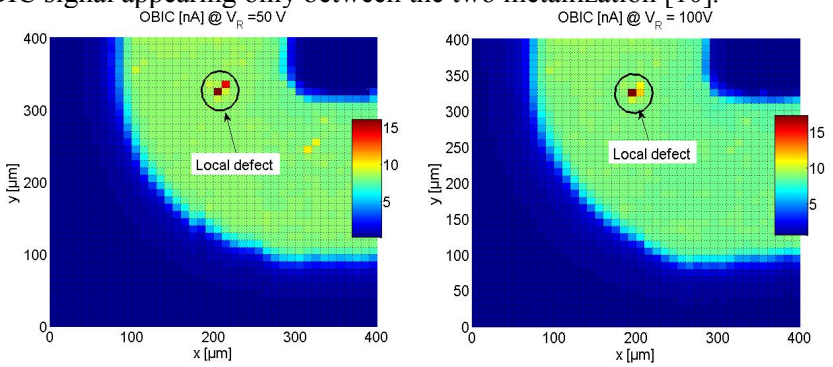

Figure 8. 2D-OBIC cartography on b-structure diode presenting a local defect (structure b) using the green laser.

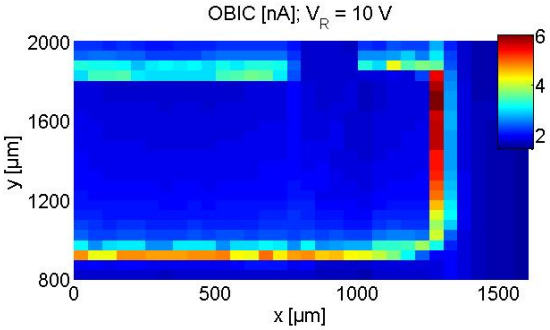

Figure 9. 2D-OBIC cartography on Schottky GaN diode (structure c) for a reverse voltage of 10 V using the UV laser.

Figure 10 shows results of OBIC measurements realized on Schottky diamond diodes. These measurements are performed using UV laser source. Preliminary results under low voltage biasing (V_R = 10 V) show an OBIC signal measured when the beam illuminates the ring around the Schottky contact. This latter being very thin is transparent to the optical beam in some regions, so an OBIC signal is observed under the metallization. Comparing photon energy (3.56 eV) and the bandgap of the diamond (5.45 eV) leads to deduce that two-photon absorption dominates in this case.

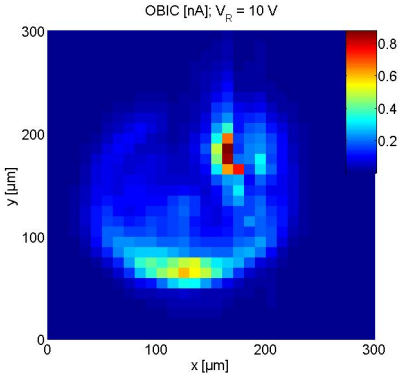

Figure 10. 2D-OBIC cartography on Schottky diamond diode (structure d) for a reverse voltage 10 V using the UV laser).

Minority carrier lifetime

Lifetime of charge carriers is a key parameter to predict the static and dynamic losses of a junction. They are defined as the mean duration before the excess minority charge carriers recombine. High minority carrier lifetime allows a low resistance when the device is conducting. However, very high carrier lifetime leads to slow switching and then to increase switching losses. OBIC technique is used to determine minority carrier lifetime in 4H-SiC [11]. JTE protected PN diode (structure b) presents DUT for these measurements. At the edge of the JTE layer, the junction is supposed to be vertical, and the minority charge carriers are holes. When the laser beam scans the diode, the OBIC measured at the edge of the JTE decreases as a function of the minority carrier diffusion length L_{dp} as shown in Eq. 4.

$$\mathrm{OBIC}(x) = \mathrm{u}\exp\left(-\frac{x}{L_{dp}}\right) \qquad \text{Eq. 4}$$

where u is the optical generation rate.

Minority carrier lifetime τ_p is related to L_{dp} and the diffusion coefficient of holes D_p as shown in Eq. 5.

$$\tau_p = \frac{{L_{dp}}^2}{D_p} = \frac{q{L_{dp}}^2}{kT\mu_p} \qquad \text{Eq. 5}$$

where k is Boltzmann constant, T the temperature, q the electron charge and μ_p the hole mobility.

Figure 11 shows the logarithm of OBIC ln(OBIC) vs. the beam position signal for voltages between 0 and 700 V. At the edge of the JTE, the slope of ln(OBIC) varies between 0.0784 μm^{-1} at 0 V and 0.067 μm^{-1} at 700V (it is almost constant for voltages between 100 and 700V). The measured point at 0 V is then rejected and the slope average for other voltage is of 0.06787 μm^{-1}. Referring to Eq. 4, this value is the inverse of L_{dp}, so the

diffusion length of holes is then 14.7 µm. Using Eq. 5 with hole mobility of 115 $cm^2.V^{-1}s^{-1}$, the lifetime of holes found is of 730 ns [12].
This value of hole lifetime is in good agreement with the results of Ivanov published in 1999 using OCVD method (680 ns at 300K) [13]. The found lifetime of holes is not contradictory with the results published in [14] where two dimensional cartographies were realized on 125 mm diameter 4H-SiC wafer using µ-PCD and TRPL techniques. Results show a charge carrier lifetime between 0.5 and 6 µs.

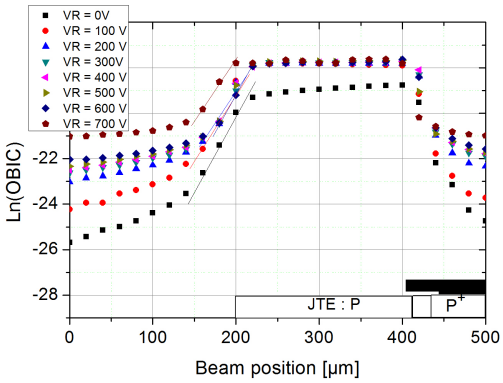

Figure 11. ln(OBIC) vs. the beam position for $0 \leq V_R \leq 700$ V (structure b), using the green laser).

Determination of ionization rates

Determination of ionization rates is essential to predict breakdown voltage of devices. They are defined as the number of generated charge carriers by collisions per length unit from one charge carrier. They are used in numerical simulators when modeling devices. OBIC method is used to determine multiplication coefficient M which is defined as the ratio between OBIC and a voltage V and a reference voltage V_0 (where there is no multiplication). Eq. 6 shows the expression of M.

$$M(V) = \frac{OBIC(V)}{OBIC(V_0)} = \frac{M_n J_n(z_p) + M_p J_p(z_n) + M_{SCR} J_{SCR}}{OBIC(V_0)} \quad \text{Eq. 6}$$

where M_n (M_p, M_{SCR}) is electron (hole, SCR) multiplication coefficient, J_n and J_p are minority carrier currents at the edges of the SCR, J_{SCR} is the photo-generated current inside the SCR (figure 1). M_n, M_p, M_{SCR} depend on the ionization rates, their expressions are given in [15]. Ionization rates α_p (for holes) and α_n (for electrons) are given by Eq. 7 [16].

$$\alpha_{n,p} = A_{n,b} \exp\left(-{}^{B_{n,p}}/_{E}\right) \quad \text{Eq. 7}$$

where $A_{n,b}$ and $B_{n,p}$ are constants to be determined and E is the electric field.
OBIC measurements are realized on diodes of structure a, and experimental multiplication curve (inside the optical window) is found by considering V_0 = 1 V. Ionization rates parameters are then adjusted to fit theoretical curve of M with experimental one by minimizing an error function ΔM [15, 17]. Table 2 displays the values of $A_{n,b}$ and $B_{n,p}$ for 4H-SiC using both of laser sources (and then single- and two-photon absorption processes). Figure 12 shows ionization rates vs. the inverse of electric field for 4H-SiC. Comparison shows that the curves are close when using green or UV laser.

Table 2. Parameters of ionization rates of 4H-SiC using OBIC method with two different wavelengths [15, 17].

	UV laser	**Green laser**	**Experimental**
A_n [10^6 cm^{-1}]	0.99	1.11	
B_n [10^7 $V.cm^{-1}$]	1.29	1.22	
A_p [10^6 cm^{-1}]	1.61	1.71	
B_p [10^7 $V.cm^{-1}$]	1.15	1.18	
ΔM	1.824	0.724	
V_{BR} [V]	62.2	59.2	58.8
E_C [$MV.cm^{-1}$]	4.9747	4.9036	

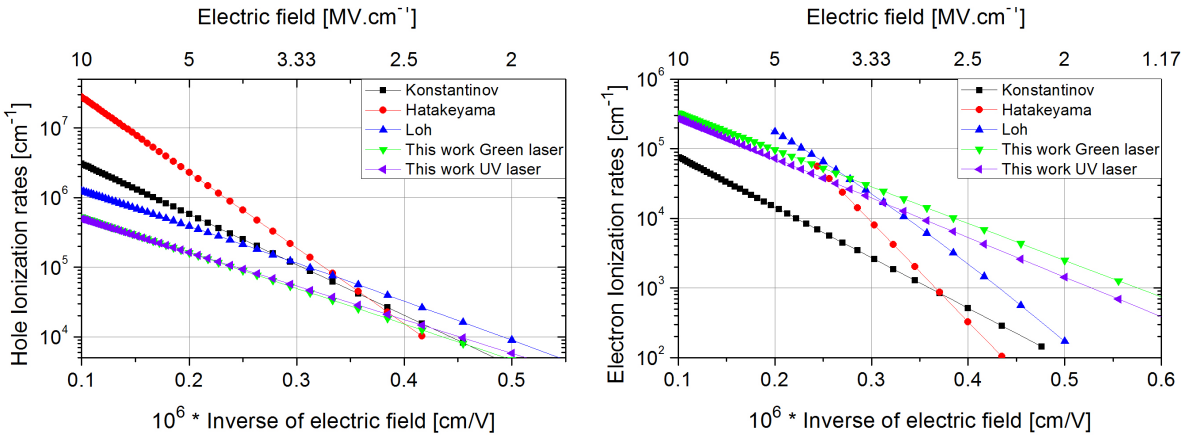

Figure 12. Ionization rates vs. inverse of electric field for 4H-SiC using OBIC method with single- and two-photon absorption process, and compared to other authors.

Figure 12 displays also ionization rates vs. inverse of the electric field found by many authors [17]. Comparison shows that the hole's ionization rates α_p are greater than electron's ionization rates α_n (as the other authors) but the ratio α_p/α_n is about twice (much smaller than the published results). Difference found between the authors is due to the doping levels of DUTs and the method used to extract ionization rates. Each result is applicable for a range of electric field; note that the found results in this work are applicable only for high electric field range (3-5 MV.cm^{-1}). In silicon, electron's ionization rates are higher than hole's ionization rates. In silicon carbide, some explanations are given by Konstantinov [18]. The discontinuity of the electron energy spectrum for motion along the c-axis makes very difficult for an electron to reach the ionization threshold without collision with phonon or tunneling. That is contradictory with the lucky electron model (Shockley model, for low electric fields). Another explanation is that the Bloch oscillations have a high impact on electrons and contribute to decrease their energy under the threshold for impact ionization.

Temperature dependence of 4H-SiC ionization rates

Other OBIC measurements are realized on diodes of structure a, in order to study their behavior under high variable temperatures. Such a study allows knowing the reliability of the devices when working in different environment conditions. Reverse electric characteristics I-V are measured for a temperature range going from 100 K up to 450 K. Measurements show a little increase of knockdown voltage (about 0.25 V per 100 K). OBIC measurements are then realized at the diameter of the diode using UV laser. Measurements show that the level of OBIC current increases with temperature (figure 13). Multiplication curves are realized by measuring OBIC signal inside the optical window. Comparison of ionization rates shows a little increase of hole's ionization rates and a little decrease of electron's ionization rates for low temperatures (< 300 K). For higher temperatures, both (electrons and holes) ionization rates are almost constant (figure 14). Table 3 resumes the values of A_n and B_n found for different temperatures [15].

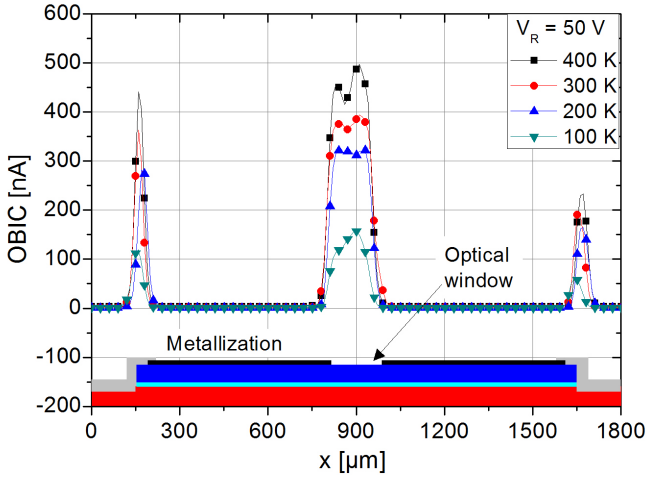

Figure 13. OBIC signal vs. beam position at 50 V for different temperatures.

The behavior of electron's ionization coefficients α_n is similar to that of electrons in silicon devices. For holes, the behavior at temperature higher than 300 K is temperature independent, which is in agreement with results found by Niwa et al. [19]. At lower temperature than 300 K, the small increase of α_p with temperature is not explained yet.

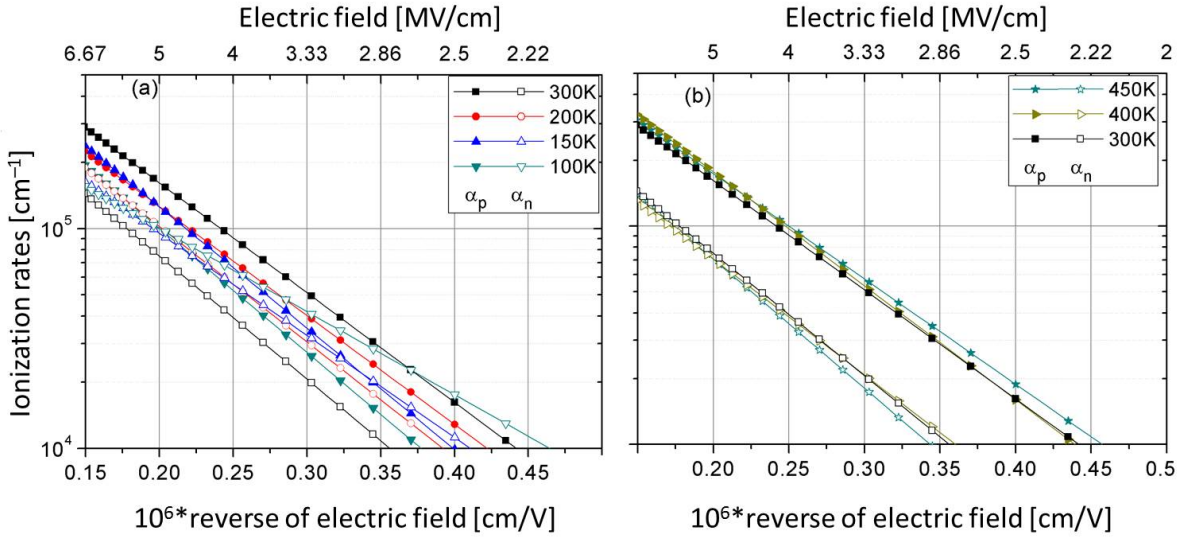

Figure 14. 4H-SiC ionization rates vs. reverse of electric field for temperature ranging between 100 and 450 K.

Table 3. Temperature dependence of ionization rates [15].

Temperature [K]	**100**	**150**	**200**	**250**	**300**	**350**	**400**	**450**
A_n [10^6 cm^{-1}]	0.57	0.81	1.15	1.04	0.99	0.87	0.81	1.07
B_n [10^7 $V.cm^{-1}$]	0.87	1.07	1.21	1.36	1.29	1.11	1.22	1.36
A_p [10^6 cm^{-1}]	1.35	1.59	1.23	1.76	1.61	1.72	1.95	1.6
B_p [10^7 $V.cm^{-1}$]	1.3	1.27	1.14	1.14	1.15	1.26	1.2	1.11

Conclusion

Wide bandgap semiconductors become the object of recent studies in the power electronic domain. In this paper, OBIC (Optical Beam Induced Current) method is used to determine electronic characteristics of 4H-SiC. It is applied to reverse biased bipolar and Schottky diodes. It is based on measuring and analyzing induced current of charge carriers generated by photon absorption inside the space charge region.

2D-OBIC cartographies are realized on 4H-SiC bipolar diodes, and GaN and diamond Schottky diodes using two laser sources with two different wavelengths (UV beam and green beam). Two-photon absorption process is investigated in case of optical generation of charge carriers in 4H-SiC using green laser, and generation in diamond using UV laser.

OBIC cartographies display an image of the electric field. They are helpful to study the performance of junction lateral protections and/or to detect material defects. This paper shows that OBIC technique is also used to determine minority carrier lifetime. Lifetime of holes in 4H-SiC is found and it is of 730 ns. OBIC measurements are used to determine ionization rates of 4H-SiC. These characteristics are key parameters to predict device behavior when it is reverse biased. They are used in numerical simulators to model devices before the conception phase.

These two experimental benches are under development, some transient measurements are realized since both laser sources are pulsed. Such measurements allow determining carrier lifetime by coupling measurements with numerical simulation. Additional work will be provided to make OBIC measurements under higher voltages, so FUG power supply (allowing voltage up to 12.5 kV) will be mounted on the experimental bench.

References

[1] Ryu S R, Cheng L, Dhar S, Capell C, Jonas C, Clayton J, Donofrio M, O'Loughlin M, Burk A, Agarwal A and Palmour J 2012 *Materials Science Forum* **717-720** 1135-1138

[2] Ejebjork N, Zirath H, Bergman P, Magnusson B and Rorsman N 2011 *Materials Science Forum* **679-680** 629-632

[3] http://www.cree.com/, "CREE"

[4] http://www.st.com/web/en/home.html, "ST"

[5] Kaji N, Niwa H, Suda J and Kimoto T 2014 *Materials Science Forum* **778-780** 832-835

[6] Goeppert-Mayer M 1931 *Ann. Phys.* **9** 273
[7] Hamad H, Raynaud C, Bevilacqua P, Tournier D, Vergne B and Planson D 2014 Optical Beam Induced Current Measurements Based on Two-Photon Absorption Process in 4H-SiC Bipolar Diodes *Applied Physics letters* **104** 082102
[8] Lazar M, Jomard F, Nguyen D M, Raynaud C, Pâques G, Scharnholz S, Tournier D and Planson D 2012 *Materials Science Forum* **717-720** 885-888
[9] Hamad H, Bevilacqua P, Raynaud C and Planson D 2014 *10th Conference on Ph. D. Research in Microelectronics and Electronics PRIME*, Grenoble, France, June 30 – July 03.
[10] Hamad H, Bevilacqua P, Planson D, Raynaud C, Tournier D, Vergne B, Lazar M and Brosselard P 2015 *EPJAP* **71** No 2 20101
[11] Flohr T and Helbig R 2008 *Journal of Applied Physics* **615-617** 703
[12] Hamad H, Raynaud C, Bevilacqua P and Planson D 2015 *International Semiconductor Conference CAS*, Sinaia, Romania, October 12-14
[13] Ivanov P A, Levinshtein M E, Irvine K G, Kordina O, Palmour J W and Rumyantsev S L 1999 *Electronic Letters*, **35** No. 16, 1382-1383
[14] Kallinger B, Rommel M, Lilja L, Ul Hassan J, Booker I, Janzén E and Bergman P *2014 Materials Science Forum* **778-780** 301-3014
[15] Hamad H, Raynaud C, Bevilacqua P, Scharnholz S and Planson D 2015 *Material Science Forum* **821-823** 223-226
[16] Chynoweth A G 1960 *Journal of Applied Physics* **95** No. 7 1161
[17] Hamad H, Raynaud C, Bevilacqua P, Scharnholz S, Vergne B and Planson D 2016 *Material Science Forum* **858** 245-248
[18] Konstantinov A.O. et al. 1997, *Appl. Phys. Lett.* **71**, 90-92
[19] Niwa H, Suda J. and Kimoto T, 2014 *Materials Science Forum* **778-780** 461-466

Acknowledgment
Authors thank Dr. Vergne Bertrand and Dr. Scharnholz Sigo from ISL (Research Institute of Saint-Louis) for helpful discussions and permitting us to realize many measurements at ISL.